DOI: 10.1534/genetics.109.101162

Detection of Protein–Protein Interactions Through Vesicle Targeting

Jacob H. Boysen,* Saranna Fanning,*,† Justin Newberg,‡ Robert F. Murphy‡,§,,†† and Aaron P. Mitchell*,††,[1]**

**Department of Microbiology and Institute of Cancer Research, Columbia University, New York, New York 10032, †Department of Microbiology, University College Cork, Cork, Ireland, ‡Center for Bioimage Informatics and Department of Biomedical Engineering, Carnegie Mellon University, Pittsburgh, Pennsylvania 15213, §Lane Center for Computational Biology and Department of Machine Learning, Carnegie Mellon University, Pittsburgh, Pennsylvania 15213, **External Fellow, Freiburg Institute for Advanced Studies, University of Freiburg, 79104 Freiburg, Germany and ††Department of Biological Sciences, Carnegie Mellon University, Pittsburgh, Pennsylvania 15213*

Manuscript received January 26, 2009
Accepted for publication March 19, 2009

ABSTRACT

The detection of protein–protein interactions through two-hybrid assays has revolutionized our understanding of biology. The remarkable impact of two-hybrid assay platforms derives from their speed, simplicity, and broad applicability. Yet for many organisms, the need to express test proteins in *Saccharomyces cerevisiae* or *Escherichia coli* presents a substantial barrier because variations in codon specificity or bias may result in aberrant protein expression. In particular, nonstandard genetic codes are characteristic of several eukaryotic pathogens, for which there are currently no genetically based systems for detection of protein–protein interactions. We have developed a protein–protein interaction assay that is carried out in native host cells by using GFP as the only foreign protein moiety, thus circumventing these problems. We show that interaction can be detected between two protein pairs in both the model yeast *S. cerevisiae* and the fungal pathogen *Candida albicans*. We use computational analysis of microscopic images to provide a quantitative and automated assessment of confidence.

THE ability to detect protein–protein interactions rapidly and systematically has driven our understanding of gene function by implicating new proteins in key biological processes and by defining interpathway communication mechanisms (Cusick *et al.* 2005; Parrish *et al.* 2006). The clear value of protein–protein interaction information has prompted the development of many different genetic and biochemical approaches to test for interaction (Berggard *et al.* 2007). Genetic approaches, such as the two-hybrid assay (Fields and Song 1989), facilitate large-scale screening so that diverse protein pairs and growth conditions can be sampled (Parrish *et al.* 2006; Tarassov *et al.* 2008). Two hybrid assays are typically carried out in surrogate hosts *Saccharomyces cerevisiae* or *Escherichia coli*, which use the universal genetic code. However, many organisms use nonstandard genetic codes (Knight *et al.* 2001), making surrogate hosts unwieldy for heterologous protein expression. This issue can be overcome with a native host-based protein interaction assay, such as we describe here.

The interaction assay that we present is built upon properties of the highly conserved **e**ndosomal **s**orting **c**omplex **r**equired for **t**ransport (ESCRT). ESCRT comprises 10 subunits, including Snf7/Vps32, that are transiently associated with the cytoplasmic face of endocytic vesicles (reviewed in Hurley and Emr 2006). ESCRT is dissociated through the action of the Vps4 ATPase; Vps4 defects cause accumulation of ESCRT-containing vesicles called class E compartments (Babst *et al.* 1997, 1998; Obita *et al.* 2007).

The assay is a test for reassignment of fusion protein localization. One fusion protein has an N-terminal segment chosen by the investigator (Yfg1 protein) fused to the ESCRT subunit Vps32. The Yfg1-Vps32 fusion serves as a bait protein that is targeted to endocytic vesicle surfaces. The second fusion protein has another N-terminal segment chosen by the investigator (Yfg2 protein) fused to GFP. The Yfg2-GFP fusion serves as a prey protein whose targeting to endocytic vesicles depends upon interaction with the bait. The assay is conducted in a *vps4* mutant host strain (Babst *et al.* 1998), which promotes vesicular accumulation of Vps32. A positive interaction between the fusion proteins results in the targeting of GFP to vesicles, yielding bright punctate signals when cells are viewed with fluorescence microscopy. Microscopic images are analyzed through computational methods to arrive at a confidence value for the interaction. Because the assay system captures protein complexes on vesicle surfaces, we refer to it as the **v**esicle **c**apture **i**nteraction (VCI) assay.

Supporting information is available online at http://www.genetics.org/cgi/content/full/genetics.109.101162/DC1.

[1]*Corresponding author:* Department of Biological Sciences, Carnegie Mellon University, 4400 Fifth Ave., MI 741 Pittsburgh, PA 15213. E-mail: apm1@andrew.cmu.edu

TABLE 1

Primer sequences

Primer name	Sequence (5′–3′)
pRS314.GFP F	aagcttgatatcgaattcctgcagcccgggggatccactagttctagagcggccgccaccGGTCGACGGATCCCCGGGTT
pRS314.GFP R	acgacgttgtaaaacgacggccagtgaattgtaatacgactcactatagggcgaattggaTCGATGAATTCGAGCTCGTT
314 cloning F	ggatccactagttctagagcggccgccacc
314 cloning R	GTTAATTAACCCGGGGATCCGTCGACC
GFPtoSNF7 F	ACGCTGCAGGTCGACGGATCCCCGGGTTAATTAACtggtcatcacttttggttgg
GFPtoSNF7 R	TCATAAGAAATTCGCTTATTTAGAAGTGGCGCGCCtcaaagccccatttctgcttg
HIS5toLEU2 F	TACAGTTCTCACATCACATCCGAACATAAACAACCatgtctgcccctaagaagatc
HIS5toLEU2 R	CTTGAAAACAAGAATCTTTTTATTGTCAGTACTCTttaagcaaggattttcttaac
GFP.URA3 PGEMT F	GGTGGTGGTTCTAAAGGTGAAGAATTATT
GFP.URA3 PGEMT R	TCTAGAAGGACCACCTTTGATTG
CaSNF7 F	ACGCTGCAGGTCGACGGATCCCCGGGTTAATTAACTGGGGATATTTTTTTGGAGGA
CaSNF7 R	TCATAAGAAATTCGCTTATTTAGAAGTGGCGCGCCTCATAATCCCATTTCAGCTTG
CaHIS1 F	TACAGTTCTCACATCACATCCGAACATAAACAACCTGTGGAATTGTGAGCGGATA
CaHIS1 R	CTTGAAAACAAGAATCTTTTTATTGTCAGTACTTTCCCAGTCACGACGTT
CaPBS2 GFP F	GTTCAATCATTATTGAGAAACAAAGTGAAGGCTCCGGCATTACATAGAGGTGGTTTACA AAAAGTGAATAGAAGCTTTCTTAATAATCATGGTGGTGGTTCTAAAGGTGAAGAATTATT
CaPBS2 GFP R	GTGTTTGTGTTAGTTTGTTAGTTTGTTTATTTATTTGTTTGTTTCTATATAATA TACTGTTT ATAATACAGCCCAATAACCTGGGCTTCATATTCATCTAGAAGGACCACCTTTGATTG
CaHOG1 pRSfus F	GGATCCACTAGTTCTAGAGCGGCCGCCACCTTTCCGTTAAAGTGTCCACTT
CaHOG1 pRSfus R	GTT AAT TAA CCC GGG GAT CCG TCG ACC AGC TCC GTT GGC GGA ATC CAA
CaSNF1 GFP F	CTAGATGAAGTTGGGTCATTCTCTGCTTATCCTTTCTTACATTTAGCTACTAGA TTAATTAT GGAATTAGCCGTAAATAGTCAAAGTGGAGGTGGTGGTTCTAAAGGTGAAGAATTATT
CaSNF1 GFP R	GGCGTAAGAAATCCAAAAAATGGGTTGTGAATTTATCATACATATTACATATCTGCTGACATCCA ATCTAAGCTAGTACTTACTTACTTTATTTCTAGAAGGACCACCTTTGATTG
CaSNF4 pRSfus F	GGATCCACTAGTTCTAGAGCGGCCGCCACCTGAATTGAATGTAAAAGAAGA
CaSNF4 pRSfus R	GTTAATTAACCCGGGGATCCGTCGACCATCTTCTCCAAATAATATGTA

MATERIALS AND METHODS

Strains, plasmids, and growth conditions: *S. cerevisiae* strain JBY357 (*MAT***a** *his3*Δ*1 leu2*Δ*0 met15*Δ*0 ura3*Δ*0 vps4*Δ*::URA3*) was constructed using PCR-directed deletion of the *VPS4* gene in parent strain BY4741 (*MAT***a** *his3*Δ*1 leu2*Δ*0 met15*Δ*0 ura3*Δ*0*), as previously described (Boysen and Mitchell 2006). *Candida albicans* strains BWP17 (*ura3*Δ*::*λ *imm434/ura3*Δ*::*λ*imm434 arg4::hisG/arg4::hisG his1::hisG/his1::hisG*) and SAL2-4F (*ura3*Δ*::*λ *imm434/ura3*Δ*::*λ*imm434 arg4::hisG/arg4::hisG his1::hisG/his1::hisG vps4*Δ*::dpl200/vps4*Δ*::dpl200*) have been described (Wilson *et al.* 1999; Lee *et al.* 2007).

Plasmids were created using *in vivo* recombination methods (Ma *et al.* 1987; Raymond *et al.* 1999). Plasmid pJB300 was created by integrating the *GFP(S65T)-HIS3MX6* cassette from pFA6a-*GFP(S65T)-HIS3MX6* into the multiple cloning site (MCS) of pRS314. The cassette was initially amplified using primers pRS314 GFP F and pRS314 GFP R (for all primer sequences, see Table 1) against the pFA6a plasmid template and cotransformed with *Not*I-/*Sac*I-linearized plasmid pRS314. This strategy integrates the GFP-coding region of the cassette 3′ of the *Not*I site and allows the majority of the MCS to be retained. Approximately 10 bp of pRS314 sequence (flanking the *Sac*I site, bp +1890 to +1900) was lost during the *in vivo* recombination event. Plasmids were recovered in *E. coli*, characterized, and sequenced. Plasmid pJB302, harboring a *VPS32 scLEU2* cassette, was derived from pJB300 in two steps. The *VPS32* gene was amplified from plasmid with primers GFPtoSNF7 F and GFPtoSNF7 R. The resulting PCR was cotransformed with pJB300 and linearized within the GFP-coding region by digestion with *Nde*I. The resulting plasmid, pJB301, was converted to Leu+ using primers HIS5toLEU2 F and HIS5toLEU2 R against pRS315 template. The PCR and pJB301, linearized within the *HIS3MX6* coding region with *Sph*I digestion, were cotransformed, and plasmids were recovered and characterized. pJB300 and pJB302 were utilized as both PCR templates using the existing pFA6-directed primers for genomic integration and as backbones for subsequent plasmid constructions. Plasmids harboring *PBS2*, *HOG1*, *SNF1*, and *SNF4* were constructed using *in vivo* recombination into pJB300 and pJB302. Primers were constructed to incorporate 1 kb 5′ upstream promoter (or, if necessary, just 3′ of any adjacent coding ORF) and the coding region of interest, less the stop codon. Flanking overhang sequences (from primers 314 cloning F and 314 cloning R; Table 1) were appended to gene-specific primers to allow subsequent integration of PCR into *Not*I-linearized pJB300 or pJB302 by *in vivo* recombination. Plasmids were retrieved and characterized as above.

Plasmid pJB407 was constructed by insertion of a GFP-URA3 cassette (Gerami-Nejad *et al.* 2001) into the pGEMT vector following the manufacturer's instructions (Promega). Subsequent GFP fusions used PCR amplification with gene-specific primers (~100 bp homologous to the gene of interest plus 23–29 bp homologous to the GFP cassette) followed by PCR-mediated transformation directed to the chromosomal locus of the gene of interest in wild-type strain BWP17 or the *vps4* mutant SAL2-4F (Lee *et al.* 2007).

pJB408, which carries *CaSNF7* and *CaHIS1* on a pRS314 *scTRP1* backbone, was constructed from plasmid pJB300 (see above) using two rounds of *in vivo* recombination. First, using primers CaSNF7 F and CaSNF7 R, the complete *caSNF7* sequence lacking a start codon was amplified and inserted in place of the GFP-coding sequence. Second, using primers

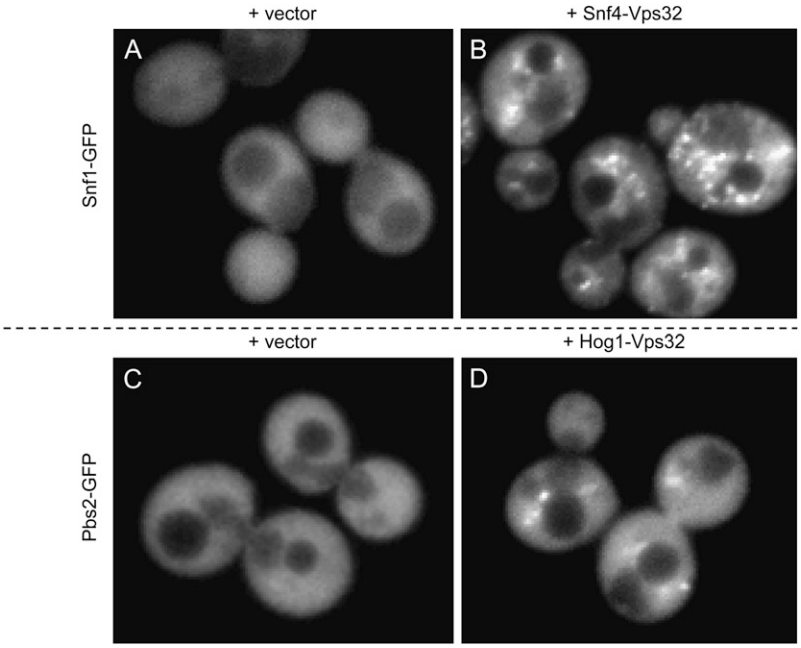

FIGURE 1.—VCI assay for *S. cerevisiae* Snf1:Snf4 and Pbs2:Hog1. An *S. cerevisiae vps4*Δ strain was transformed with a Snf1-GFP fusion plasmid and either a Vps32 vector (A) or a Snf4-Vps32 fusion plasmid (B). The *vps4*Δ strain was independently transformed with a Pbs2-GFP fusion plasmid and either a Vps32 vector (C) or a Hog1-Vps32 fusion plasmid (D). GFP fluorescence images are shown.

CaHIS1 F and CaHIS1 R, the *caHIS1* sequence was amplified and inserted into the *CaSNF7* plasmid pJB401, with the *caHIS1* sequence completely replacing the *Schizosaccharomyces pombe his5*+ sequence. The resulting plasmid pJB408 contains a 5′ cloning site with a unique *Not*I site; this site was subsequently used, in conjunction with a homologous linking sequence appended to gene-specific primers, to direct the *in vivo* recombination of fusions to *SNF7*. Genes were amplified with either 5′ sequence up to the neighboring gene or with 1 kb, whichever was least. Thereafter, using a unique *Nru*I site in the *CaHIS1* sequence, Snf7 fusions were targeted to the chromosomal *caHIS1* locus in the GFP+ (wild type and Δ*caVPS4*/Δ*caVPS4*) strains isolated above.

Yeast growth media (YPD and SC) were of standard composition (KAISER *et al.* 1994). All plates and liquid cultures were incubated at 30°.

Microscopy: Imaging was performed at room temperature on a Nikon Eclipse E800 widefield fluorescence microscope with a Nikon Plan Apo ×100 1.4 objective (Melville, NY) and a Hamamatsu Orca100 digital CCD Camera (Bridgewater, NJ). Images were acquired with OpenLab Improvision software. Staining with *N*-(3-triethylammoniumpropyl)-4-(*p*-diethylaminophenylhexatrienyl)-pyridinium dibromide (FM4-64, purchased from Molecular Diagnostics, Chicago) was performed as described previously (BOYSEN and MITCHELL 2006).

Quantitative image measurement: Raw fluorescence micrographs of the GFP signal were processed in Matlab 7.4. These 8-bit grayscale images were corrected for background by subtracting the most common pixel value, and then each image was stretched to 64 gray levels. For each of these processed images, four gray-level co-occurrence matrices were calculated to measure horizontal, vertical, left-diagonal, and right-diagonal nearest neighbor occurrences. Thirteen Haralick texture features were calculated from each of these resulting matrices, and these features were averaged in the horizontal/vertical and left-diagonal/right-diagonal directions, giving 26 texture features (CHEBIRA *et al.* 2007). Additionally, cumulative gray-level frequency features were calculated from the stretched images. For each image, a histogram was calculated on all pixels with intensity greater than zero, and the cumulative frequency of pixels at each of 62 grayscale values was used as features (the cumulative frequency for pixel value 63 is ignored because it is always 1). See http://murphylab.web.cmu.edu/software/ and http://murphylab.web.cmu.edu/data/ for analysis programs and raw image files.

RESULTS

***S. cerevisiae* VCI assay:** The VCI assay platform was first tested in *S. cerevisiae* because of the ease of manipulation. We tested two protein-kinase-related complexes, Snf1:Snf4 and Pbs2:Hog1. Snf1 is the *S. cerevisiae* AMP-activated protein kinase, and Snf4 is its regulatory gamma subunit (SCHULLER 2003). Snf1:Snf4 interaction was detected in the first published two-hybrid assay (FIELDS and SONG 1989). Pbs2 and Hog1 are the MAPKK and MAPK, respectively, that are required for the *S. cerevisiae* high osmolarity response (HOHMANN 2002). Interaction between Hog1 and Pbs2 is well documented (POSAS and SAITO 1997) but has never been detected in published two-hybrid assays or other genetic protein–protein interaction tests.

*S. cerevisiae vps4*Δ cells carrying a Snf1-GFP fusion plasmid, along with the Vps32 fusion vector, gave diffuse cytoplasmic fluorescence (Figure 1A and supporting information, Figure S4). As seen for most cytoplasmic GFP fusions in *S. cerevisiae* (HUH *et al.* 2003), there was exclusion from the vacuole. The presence of both Snf1-GFP and Snf4-Vps32 fusion plasmids in the *vps4*Δ cells yielded punctate fluorescent foci (Figure 1B and Figure S3). Similar foci were observed when the GFP and Vps32 tags were reversed (*i.e.*, Snf4-GFP and Snf1-Vps32; data not shown). The foci colocalized substantially with the membrane dye FM4-64 (Figure 2), which accumulates in the endosome-derived class E compartments in *vps4*Δ mutant cells (KRANZ *et al.* 2001). Foci were rare

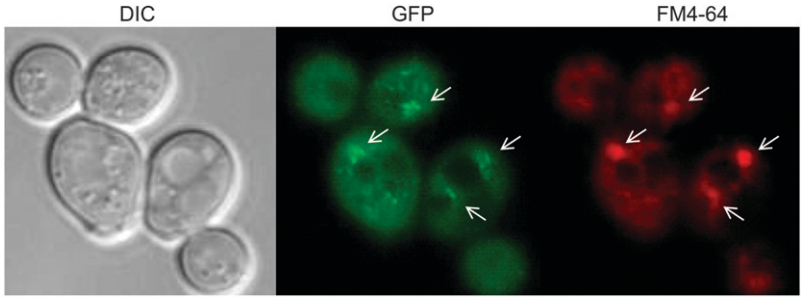

Figure 2.—Comparison of GFP localization and FM4-64 staining. An *S. cerevisiae vps4*Δ mutant host expressing both Snf1-GFP and Snf4-Vps32 was stained with membrane dye FM4-64. The dye accumulates in endosome-derived class E compartments in *vps4* mutants. DIC, GFP, and FM4-64 channels are shown. White arrows indicate regions of GFP and FM4-64 colocalization.

and relatively faint with these plasmid combinations in *VPS4* cells (see Figure S7 and Figure S8). The two findings—that foci depend upon a *vps4* mutation and that they colocalize with FM4-64-stained regions—are consistent with the idea that foci correspond to endosome-associated ESCRT complexes. The fact that GFP foci depend upon the presence of an interacting protein fused to Vps32 argues that the Vps32 fusion protein targets the GFP fusion protein to the endosome.

To determine whether VCI assays may be useful for other pairs of proteins, we carried out a similar analysis of Pbs2 and Hog1. Once again, punctate GFP foci were detected only in cells that expressed both Pbs2-GFP and Hog1-Vps32 fusions (compare Figure 1D to Figure 1C and Figure S1 to Figure S2) and were dependent upon a *vps4*Δ mutation (Figure S5). Formation of GFP foci was dependent upon interacting fusion proteins because no foci were observed when the *vps4*Δ strain carried Snf1-GFP together with Hog1-Vps32 or Pbs2-GFP together with Snf4-Vps32 (data not shown). Therefore, the VCI assay permits detection of protein–protein interaction for two pairs of *S. cerevisiae* gene products that were known to exist in complexes.

***C. albicans* VCI assay:** We sought to develop the VCI assay in *C. albicans* because there is no simple protein–protein interaction assay available for that organism. We chose the *C. albicans* protein pairs Snf1:Snf4 and Pbs2:Hog1, the orthologs of the *S. cerevisiae* protein pairs used above. In *C. albicans*, presence of the Snf1-GFP or Pbs2-GFP with the Vps32 vector yielded diffuse cytoplasmic fluorescence (Figure 3, A and C, and Figure S10 and Figure S12). However, presence of both Snf1-GFP and Snf4-Vps32, or Pbs2-GFP and Hog1-Vps32, yielded punctate GFP foci (Figure 3, B and D, and Figure S9 and Figure S11). The foci occasionally resembled ribbons or whorls, as do some class E compartments (Luhtala and Odorizzi 2004; Russell *et al.* 2006). The foci were dependent upon the *vps4*Δ/*vps4*Δ genotype (data not shown). Interaction was specific because no foci were observed in cells expressing both Pbs2-GFP and Snf4-Vps32 (Figure S13). These observations indicate that the VCI system can detect interactions between two *C. albicans* protein pairs.

Computational assessment of VCI images: Although positive and negative VCI assay images can be distinguished by eye, we sought to develop a computational image analysis strategy to arrive at a confidence level for interaction. We collected random images for strains expressing each prey fusion plus bait vector only (negative class, such as Figure 1, A and C, and Figure 3, A and C) or each prey fusion plus bait fusion (positive class, like Figures 1B, 1D, 3B, and 3D). We evaluated whether or not a classification system can distinguish them (Glory and Murphy 2007) as follows. Each image was processed to produce quantitative features that reflect the degree to which the GFP signal is contained in bright, punctate structures. The simplest approach was to identify punctate structures (if any) and measure the fraction of fluorescence contained in them. However, the heterogeneous nature of the vesicle compartments makes it difficult to identify them directly. We therefore created a series of features that calculate the fraction of fluorescence contained in pixels above a given threshold and used these in conjunction with Haralick texture features, which we previously demonstrated are valuable for analysis of subcellular patterns (Chebira *et al.* 2007). The features were calculated for each image and used to train support vector machine classifiers (Byvatov and Schneider 2003). The performance of the classifiers was evaluated using leave-one-out cross-validation. In this approach, a classifier was trained on all images except one and then tested on the remaining image; the classification process was repeated until all images had been used for testing. The class assigned by the classifier was then compared to the known class and tabulated (Table 2). For *S. cerevisiae* VCI assays, we used only 10 images/strain, and the classifier achieved performance of 80–95%. We suspect that performance was limited by the small number of images. For the *C. albicans* VCI assays, we used 20–25 images/strain and classifier performance was 90–95%. We used multivariate hypothesis tests (Chen *et al.* 2006) to determine whether the feature distributions of the positive and negative conditions were significantly different. By the Friedman–Rafsky test, all pairs of VCI positive and negative image sets were distinguished with highly significant *P*-values (Table 2). This computational analysis provides a useful approach to quantifying differences between VCI positive and negative samples.

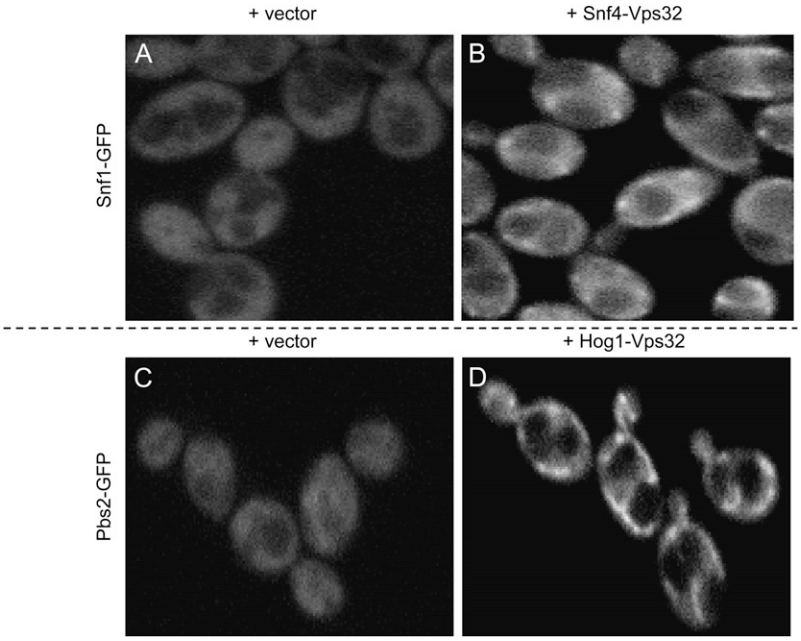

FIGURE 3.—VCI assay for C. *albicans* Snf1:Snf4 and Pbs2:Hog1. A *C. albicans vps4*Δ*/vps4*Δ strain was transformed to introduce a Snf1-GFP fusion gene and either the Vps32 vector (A) or a Snf4-Vps32 fusion gene (B). The *vps4*Δ*/vps4*Δ strain was independently transformed to introduce a Pbs2-GFP fusion gene and either the Vps32 vector (C) or a Hog1-Vps32 fusion gene (D). GFP fluorescence images are shown.

DISCUSSION

The VCI assay described here has proven workable for two protein complexes in two organisms. We expect such a native host-based assay to be particularly useful in *C. albicans* because of its nonstandard genetic code and the lack of any other genetic protein–protein interaction test at present. The assay requires only modest molecular genetic manipulation and is based upon highly conserved eukaryotic machinery. Therefore, it may be useful in many other organisms as well.

The VCI assay has several generally useful features. First, the fusion proteins are expressed from their native promoters, rather than overexpressed, so that natural stoichiometry of interacting proteins can be maintained. Second, real-time imaging may facilitate detection of transient complexes, particularly in response to environmental changes. Third, single-cell assays such as this can be powerful for detecting transient responses in asynchronous or heterogenous populations, such as those engaged in biofilm formation or sporulation. These advantages are shared with protein-fragment-complementation-based interaction assays (REMY and MICHNICK 2004). However, the VCI assay offers the additional advantage that the native *VPS32* coding region is used as one fusion partner, thus eliminating the need for codon changes before implementation in hosts with divergent genetic codes. Many GFP coding regions that function in hosts with variant genetic codes have been described (HA *et al.* 1996; CORMACK *et al.* 1997; HOSEIN *et al.* 2003).

The need for a *vps4* defect in the VCI host strain is a potential limitation of the assay because it may be difficult to disrupt genomic copies of *VPS4* in many organisms. However, Vps4 defects can also be achieved through ectopic inactivation strategies, including RNA interference or the use of a dominant-negative *VPS4* allele. Dominant-negative *VPS4-DN* alleles have been used to probe ESCRT function in genetically unwieldy cells, including human cell lines and *Leishmania major* (HISLOP *et al.* 2004; BESTEIRO *et al.* 2006; TAYLOR *et al.* 2007). Thus we expect that impairment of Vps4 function will not be a major impediment to VCI assay implementation.

For the assays presented here, computational analysis provides an objective means to compare image sets and support statistical assessment of interaction. In the longer term, computational image analysis yields an avenue for scaling up the VCI assay. It permits use of automated microscopy methods (GLORY and MURPHY 2007), so that the VCI assay may be implemented with large sample sets, such as large numbers of protein pairs or time points. Indeed, automated microscopy has been used to define prospective drug targets (PERLMAN *et al.* 2004) and to evaluate subcellular protein localization (ROQUES and MURPHY 2002; CHEN *et al.* 2007; GLORY and MURPHY 2007). Automated subcellular localization assignments have proven more sensitive than visual interpretation by human observers (ROQUES and MURPHY 2002; CHEN *et al.* 2007; GLORY and MURPHY 2007).

There are some detailed points to consider about the VCI assay. First, the brightness of our cell populations is variable, as one can see from the supplemental figures. This heterogeneity probably arises from allowing cells to settle in culture tubes before imaging; we find the most homogenous and distinct images from early to mid-logarithmic cultures that are growing actively just prior to imaging. Second, our *C. albicans* VCI signals do not resemble class E compartments (KULLAS *et al.* 2004; LEE *et al.* 2007). We suspect that their unusual appearance

TABLE 2

Quantitative assessment of VCI assay results

Organism	GFP fusion	Vps32 fusion	No. of images	Classifier output		Classifier accuracy (%)	*P*-value for positive *vs.* negative
				VCI positive	VCI negative		
S. cerevisiae	Snf1	Snf4	10	90.0	10.0	95.0	1×10^{-5}
		(vector)	10	0.0	100.0		
S. cerevisiae	Pbs2	Hog1	10	90.0	10.0	80.0	0.03
		(vector)	10	30.0	70.0		
C. albicans	Snf1	Snf4	25	96.0	4.0	95.5	6×10^{-8}
		(vector)	20	5.0	95.0		
C. albicans	Pbs2	Hog1	20	90.0	10.0	90.0	3×10^{-6}
		(vector)	20	10.0	90.0		

arises from the overall increased expression of Vps32 in these cells; the Hog1-Vps32 and Snf4-Vps32 fusions are expressed from the *HOG1* and *SNF4* promoters, respectively.

The immediate value of the VCI assay is as a protein–protein interaction test for *C. albicans*. For some time the prevailing view was that *C. albicans* gene function was largely similar to *S. cerevisiae* gene function. For example, it appeared that processes such as filamentation (Lo *et al.* 1997), pH responses (Davis 2003), cell-wall integrity (Navarro-Garcia *et al.* 2001), and basic growth and viability (see Devasahayam *et al.* 2002; Michel *et al.* 2002) were governed by the *C. albicans* orthologs of known *S. cerevisiae* pathway participants. Such a scenario placed little importance on specific tests of *C. albicans* protein–protein interaction because the expectation was that they would simply recapitulate interactions among the *S. cerevisiae* orthologs. However, that view was driven by "sampling error"; that is, *C. albicans* gene function analysis rested largely upon candidate gene approaches that in turn were based on prior *S. cerevisiae* gene discovery. More recently, the *C. albicans* community has embraced new gene discovery strategies, including the screening of heterozygous, homozygous, or conditional expression *C. albicans* mutant libraries (Bruno and Mitchell 2004; Noble and Johnson 2007), as well as candidate gene selection based upon microarray expression profiling (Garaizar *et al.* 2006; Brown *et al.* 2007) or proteomic analysis (de Groot *et al.* 2004; Kusch *et al.* 2007). These strategies have fueled the reexamination of processes conserved between *S. cerevisiae* and *C. albicans* and have supported direct inquiry into distinct biological features of *C. albicans*, such as its ability to interact with host cells, invade tissues, and form biofilms. Such studies reveal that *C. albicans* indeed uses unique genes, pathways, and networks to meet its biological needs (see, for example, Roemer *et al.* 2003; Nobile and Mitchell 2005; Bruno *et al.* 2006; Huang *et al.* 2006; Srikantha *et al.* 2006; Zordan *et al.* 2006; Martchenko *et al.* 2007; Hogues *et al.* 2008). We are now poised for mechanistic studies that will yield a basic understanding of functional relationships and, ultimately, insight into the choice of therapeutic targets.

We thank members of our labs for advice and discussion. We are grateful to Sam Lee for providing the *C. albicans vps4Δ/vps4Δ* mutant.This work was supported by National Institutes of Health grant 5R01AI070272 (A.P.M.), National Science Foundation ITR grant EF-0331657 (R.F.M.), and a National University of Ireland Travelling Studentship (S.F.).

LITERATURE CITED

Babst, M., T. K. Sato, L. M. Banta and S. D. Emr, 1997 Endosomal transport function in yeast requires a novel AAA-type ATPase, Vps4p. EMBO J. **16:** 1820–1831.

Babst, M., B. Wendland, E. J. Estepa and S. D. Emr, 1998 The Vps4p AAA ATPase regulates membrane association of a Vps protein complex required for normal endosome function. EMBO J. **17:** 2982–2993.

Berggard, T., S. Linse and P. James, 2007 Methods for the detection and analysis of protein-protein interactions. Proteomics **7:** 2833–2842.

Besteiro, S., R. A. Williams, L. S. Morrison, G. H. Coombs and J. C. Mottram, 2006 Endosome sorting and autophagy are essential for differentiation and virulence of Leishmania major. J. Biol. Chem. **281:** 11384–11396.

Boysen, J. H., and A. P. Mitchell, 2006 Control of Bro1-domain protein Rim20 localization by external pH, ESCRT machinery, and the Saccharomyces cerevisiae Rim101 pathway. Mol. Biol. Cell **17:** 1344–1353.

Brown, A. J., F. C. Odds and N. A. Gow, 2007 Infection-related gene expression in Candida albicans. Curr. Opin. Microbiol. **10:** 307–313.

Bruno, V. M., and A. P. Mitchell, 2004 Large-scale gene function analysis in Candida albicans. Trends Microbiol. **12:** 157–161.

Bruno, V. M., S. Kalachikov, R. Subaran, C. J. Nobile, C. Kyratsous *et al.*, 2006 Control of the C. albicans cell wall damage response by transcriptional regulator Cas5. PLoS Pathog. **2:** e21.

Byvatov, E., and G. Schneider, 2003 Support vector machine applications in bioinformatics. Appl. Bioinformatics **2:** 67–77.

Chebira, A., Y. Barbotin, C. Jackson, T. Merryman, G. Srinivasa *et al.*, 2007 A multiresolution approach to automated classification of protein subcellular location images. BMC Bioinformatics **8:** 210.

Chen, S.-C., T. Zhao, G. J. Gordon and R. F. Murphy, 2006 A novel graphical model approach to segmenting cell images. Proceedings of the 2006 IEEE Symposium on Computational Intelligence in Bioinformatics and Computational Biology, pp. 1–8. http://www.ieee.org.

Chen, S. C., T. Zhao, G. J. Gordon and R. F. Murphy, 2007 Automated image analysis of protein localization in budding yeast. Bioinformatics **23:** i66–i71.

Cormack, B. P., G. Bertram, M. Egerton, N. A. Gow, S. Falkow *et al.*, 1997 Yeast-enhanced green fluorescent protein (yEGFP)a reporter of gene expression in Candida albicans. Microbiology **143**(Pt. 2): 303–311.

Cusick, M. E., N. Klitgord, M. Vidal and D. E. Hill, 2005 Interactome: gateway into systems biology. Hum. Mol. Genet. **14**(Spec. No. 2): R171–R181.

Davis, D., 2003 Adaptation to environmental pH in Candida albicans and its relation to pathogenesis. Curr. Genet. **44:** 1–7.

de Groot, P. W., A. D. de Boer, J. Cunningham, H. L. Dekker, L. de Jong *et al.*, 2004 Proteomic analysis of Candida albicans cell walls reveals covalently bound carbohydrate-active enzymes and adhesins. Eukaryot. Cell **3:** 955–965.

Devasahayam, G., V. Chaturvedi and S. D. Hanes, 2002 The Ess1 prolyl isomerase is required for growth and morphogenetic switching in *Candida albicans*. Genetics **160:** 37–48.

Fields, S., and O. Song, 1989 A novel genetic system to detect protein-protein interactions. Nature **340:** 245–246.

Garaizar, J., S. Brena, J. Bikandi, A. Rementeria and J. Ponton, 2006 Use of DNA microarray technology and gene expression profiles to investigate the pathogenesis, cell biology, antifungal susceptibility and diagnosis of Candida albicans. FEMS Yeast Res. **6:** 987–998.

Gerami-Nejad, M., J. Berman and C. A. Gale, 2001 Cassettes for PCR-mediated construction of green, yellow, and cyan fluorescent protein fusions in Candida albicans. Yeast **18:** 859–864.

Glory, E., and R. F. Murphy, 2007 Automated subcellular location determination and high-throughput microscopy. Dev. Cell **12:** 7–16.

Ha, D. S., J. K. Schwarz, S. J. Turco and S. M. Beverley, 1996 Use of the green fluorescent protein as a marker in transfected Leishmania. Mol. Biochem. Parasitol. **77:** 57–64.

Hislop, J. N., A. Marley and M. Von Zastrow, 2004 Role of mammalian vacuolar protein-sorting proteins in endocytic trafficking of a non-ubiquitinated G protein-coupled receptor to lysosomes. J. Biol. Chem. **279:** 22522–22531.

Hogues, H., H. Lavoie, A. Sellam, M. Mangos, T. Roemer *et al.*, 2008 Transcription factor substitution during the evolution of fungal ribosome regulation. Mol. Cell **29:** 552–562.

Hohmann, S., 2002 Osmotic stress signaling and osmoadaptation in yeasts. Microbiol. Mol. Biol. Rev. **66:** 300–372.

Hosein, R. E., S. A. Williams, K. Haye and R. H. Gavin, 2003 Expression of GFP-actin leads to failure of nuclear elongation and cytokinesis in Tetrahymena thermophila. J. Eukaryot. Microbiol. **50:** 403–408.

Huang, G., H. Wang, S. Chou, X. Nie, J. Chen *et al.*, 2006 Bistable expression of WOR1, a master regulator of white-opaque switching in Candida albicans. Proc. Natl. Acad. Sci. USA **103:** 12813–12818.

Huh, W. K., J. V. Falvo, L. C. Gerke, A. S. Carroll, R. W. Howson *et al.*, 2003 Global analysis of protein localization in budding yeast. Nature **425:** 686–691.

Hurley, J. H., and S. D. Emr, 2006 The ESCRT complexes: structure and mechanism of a membrane-trafficking network. Annu. Rev. Biophys. Biomol. Struct. **35:** 277–298.

Kaiser, C., S. Michaelis and A. Mitchell, 1994 *Methods in Yeast Genetics.* Cold Spring Harbor Laboratory Press, Cold Spring Harbor, NY.

Knight, R. D., S. J. Freeland and L. F. Landweber, 2001 Rewiring the keyboard: evolvability of the genetic code. Nat. Rev. Genet. **2:** 49–58.

Kranz, A., A. Kinner and R. Kolling, 2001 A family of small coiled-coil-forming proteins functioning at the late endosome in yeast. Mol. Biol. Cell **12:** 711–723.

Kullas, A. L., M. Li and D. A. Davis, 2004 Snf7p, a component of the ESCRT-III protein complex, is an upstream member of the RIM101 pathway in Candida albicans. Eukaryot. Cell **3:** 1609–1618.

Kusch, H., S. Engelmann, D. Albrecht, J. Morschhauser and M. Hecker, 2007 Proteomic analysis of the oxidative stress response in Candida albicans. Proteomics **7:** 686–697.

Lee, S. A., J. Jones, Z. Khalique, J. Kot, M. Alba *et al.*, 2007 A functional analysis of the Candida albicans homolog of Saccharomyces cerevisiae VPS4. FEMS Yeast Res. **7:** 973–985.

Lo, H. J., J. R. Kohler, B. DiDomenico, D. Loebenberg, A. Cacciapuoti *et al.*, 1997 Nonfilamentous C. albicans mutants are avirulent. Cell **90:** 939–949.

Luhtala, N., and G. Odorizzi, 2004 Bro1 coordinates deubiquitination in the multivesicular body pathway by recruiting Doa4 to endosomes. J. Cell Biol. **166:** 717–729.

Ma, H., S. Kunes, P. J. Schatz and D. Botstein, 1987 Plasmid construction by homologous recombination in yeast. Gene **58:** 201–216.

Martchenko, M., A. Levitin, H. Hogues, A. Nantel and M. Whiteway, 2007 Transcriptional rewiring of fungal galactose-metabolism circuitry. Curr. Biol. **17:** 1007–1013.

Michel, S., S. Ushinsky, B. Klebl, E. Leberer, D. Thomas *et al.*, 2002 Generation of conditional lethal Candida albicans mutants by inducible deletion of essential genes. Mol. Microbiol. **46:** 269–280.

Navarro-Garcia, F., B. Eisman, E. Roman, C. Nombela and J. Pla, 2001 Signal transduction pathways and cell-wall construction in Candida albicans. Med. Mycol. **39**(Suppl. 1): 87–100.

Nobile, C. J., and A. P. Mitchell, 2005 Regulation of cell-surface genes and biofilm formation by the C. albicans transcription factor Bcr1p. Curr. Biol. **15:** 1150–1155.

Noble, S. M., and A. D. Johnson, 2007 Genetics of Candida albicans, a diploid human fungal pathogen. Annu. Rev. Genet. **41:** 193–211.

Obita, T., S. Saksena, S. Ghazi-Tabatabai, D. J. Gill, O. Perisic *et al.*, 2007 Structural basis for selective recognition of ESCRT-III by the AAA ATPase Vps4. Nature **449:** 735–739.

Parrish, J. R., K. D. Gulyas and R. L. Finley, Jr., 2006 Yeast two-hybrid contributions to interactome mapping. Curr. Opin. Biotechnol. **17:** 387–393.

Perlman, Z. E., M. D. Slack, Y. Feng, T. J. Mitchison, L. F. Wu *et al.*, 2004 Multidimensional drug profiling by automated microscopy. Science **306:** 1194–1198.

Posas, F., and H. Saito, 1997 Osmotic activation of the HOG MAPK pathway via Ste11p MAPKKK: scaffold role of Pbs2p MAPKK. Science **276:** 1702–1705.

Raymond, C. K., T. A. Pownder and S. L. Sexson, 1999 General method for plasmid construction using homologous recombination. Biotechniques **26:** 134–138, 140–131.

Remy, I., and S. W. Michnick, 2004 Mapping biochemical networks with protein-fragment complementation assays. Methods Mol. Biol. **261:** 411–426.

Roemer, T., B. Jiang, J. Davison, T. Ketela, K. Veillette *et al.*, 2003 Large-scale essential gene identification in Candida albicans and applications to antifungal drug discovery. Mol. Microbiol. **50:** 167–181.

Roques, E. J., and R. F. Murphy, 2002 Objective evaluation of differences in protein subcellular distribution. Traffic **3:** 61–65.

Russell, M. R., D. P. Nickerson and G. Odorizzi, 2006 Molecular mechanisms of late endosome morphology, identity and sorting. Curr. Opin. Cell Biol. **18:** 422–428.

Schuller, H. J., 2003 Transcriptional control of nonfermentative metabolism in the yeast Saccharomyces cerevisiae. Curr. Genet. **43:** 139–160.

Srikantha, T., A. R. Borneman, K. J. Daniels, C. Pujol, W. Wu *et al.*, 2006 TOS9 regulates white-opaque switching in Candida albicans. Eukaryot. Cell **5:** 1674–1687.

Tarassov, K., V. Messier, C. R. Landry, S. Radinovic, M. M. Serna Molina *et al.*, 2008 An in vivo map of the yeast protein interactome. Science **320:** 1465–1470.

Taylor, G. M., P. I. Hanson and M. Kielian, 2007 Ubiquitin depletion and dominant-negative VPS4 inhibit rhabdovirus budding without affecting alphavirus budding. J. Virol. **81:** 13631–13639.

Wilson, R. B., D. Davis and A. P. Mitchell, 1999 Rapid hypothesis testing with Candida albicans through gene disruption with short homology regions. J. Bacteriol. **181:** 1868–1874.

Zordan, R. E., D. J. Galgoczy and A. D. Johnson, 2006 Epigenetic properties of white-opaque switching in Candida albicans are based on a self-sustaining transcriptional feedback loop. Proc. Natl. Acad. Sci. USA **103:** 12807–12812.

Communicating editor: M. D. Rose

GENETICS

Supporting Information

http://www.genetics.org/cgi/content/full/genetics.109.101162/DC1

Detection of Protein–Protein Interactions Through Vesicle Targeting

Jacob H. Boysen, Saranna Fanning, Justin Newberg, Robert F. Murphy and Aaron P. Mitchell

DOI: 10.1534/genetics.109.101162

A

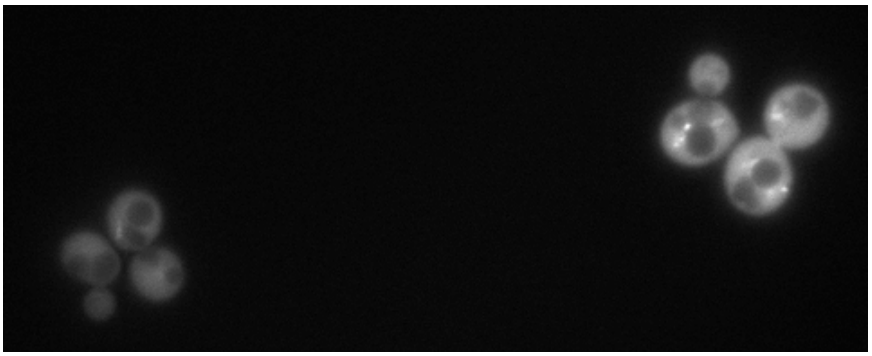

B

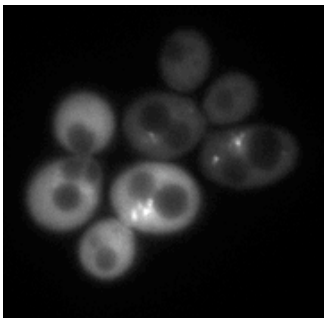

C

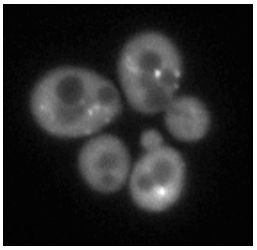

D

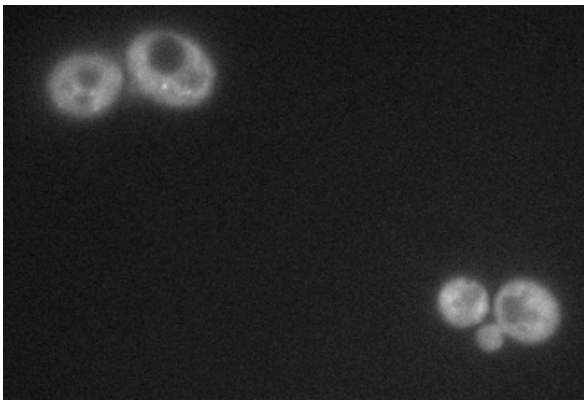

FIGURE S1.—*S. cerevisiae* PBS2GFP & HOG1VPS32 vps4-. Sets of 3-4 fields of GFP fluorescence images for *S. cerevisiae* interacting protein pairs and negative controls. All fields are shown at the same magnification.

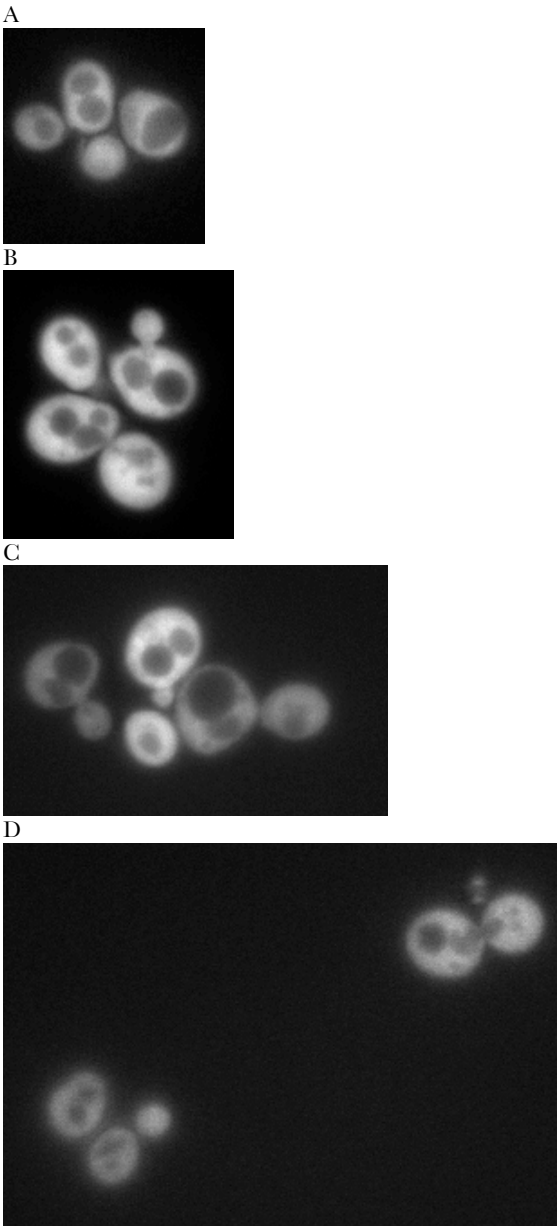

Figure S2.—*S. cerevisiae* PBS2GFP & VPS32 vps4-. Sets of 3-4 fields of GFP fluorescence images for *S. cerevisiae* interacting protein pairs and negative controls. All fields are shown at the same magnification.

A

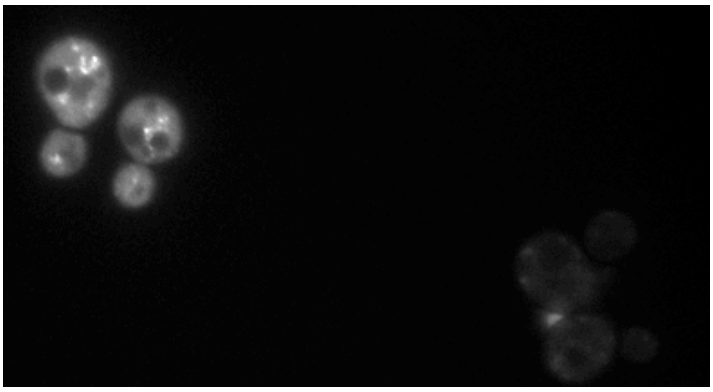

B

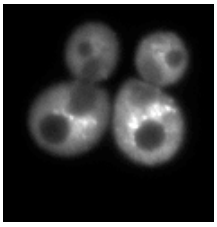

C

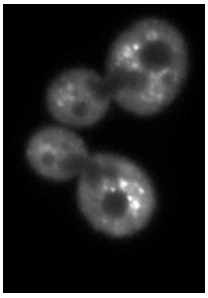

D

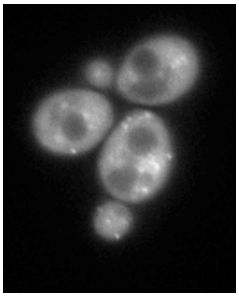

FIGURE S3.—*S. cerevisiae* SNF1GFP & SNF4VPS32 vps4-. Sets of 3-4 fields of GFP fluorescence images for *S. cerevisiae* interacting protein pairs and negative controls. All fields are shown at the same magnification.

A

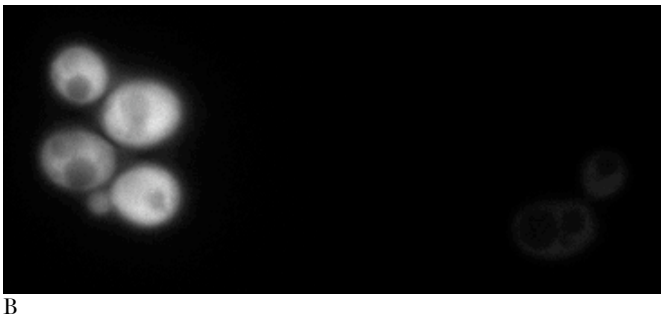

B

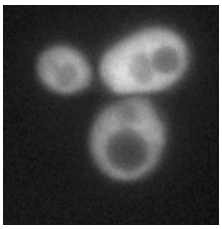

C

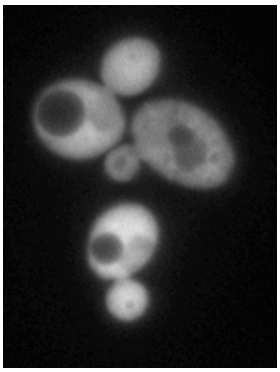

D

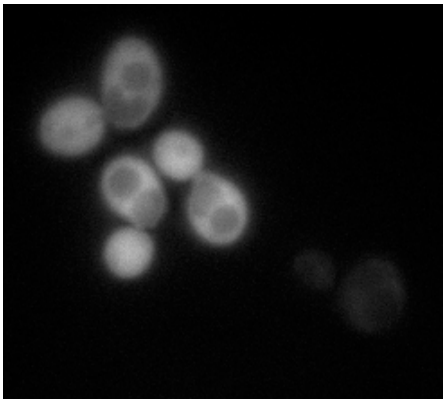

FIGURE S4.— *S. cerevisiae* SNF1GFP & VPS32 vps4-. Sets of 3-4 fields of GFP fluorescence images for *S. cerevisiae* interacting protein pairs and negative controls. All fields are shown at the same magnification.

A

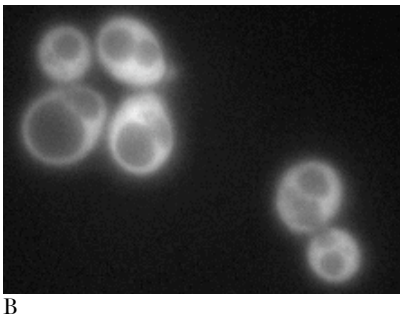

B

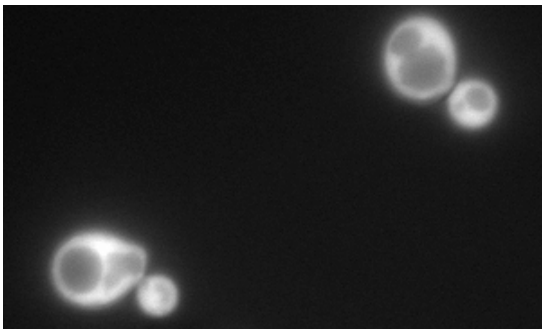

C

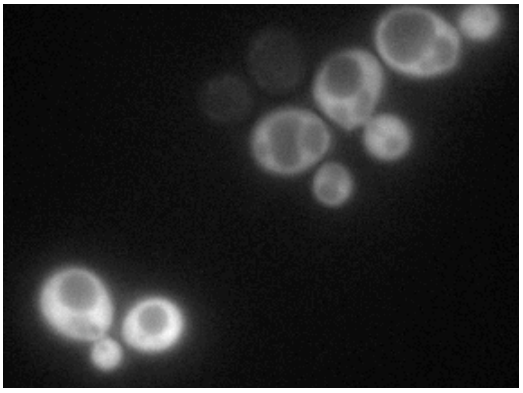

D

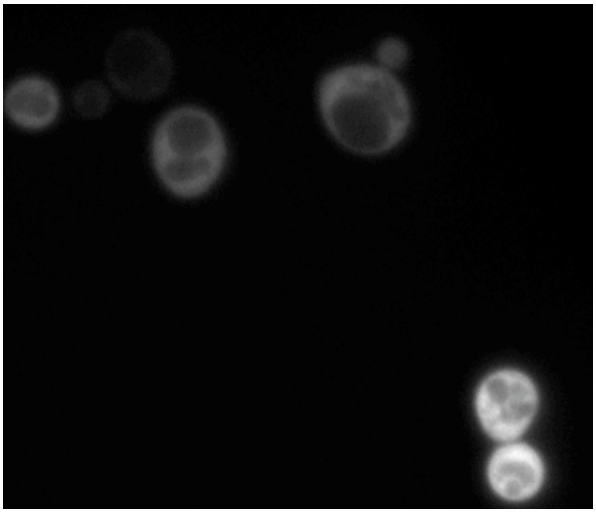

FIGURE S5.—*S. cerevisiae* PBS2GFP & HOG1VPS32 WT. Sets of 3-4 fields of GFP fluorescence images for *S. cerevisiae* interacting protein pairs and negative controls. All fields are shown at the same magnification.

A

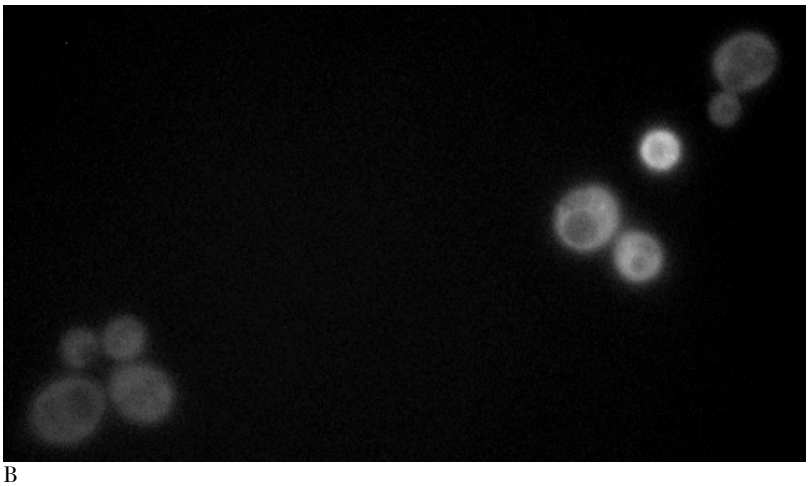

B

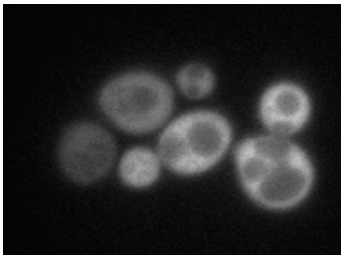

C

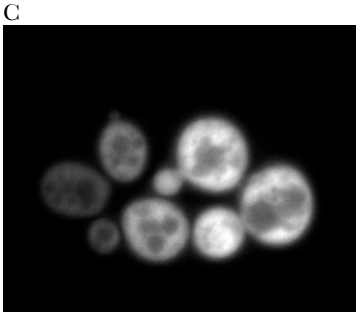

D

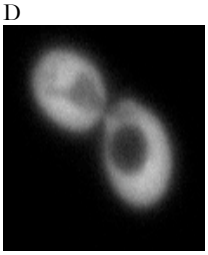

FIGURE S6.— *S. cerevisiae* PBS2GFP & VPS32 WT. Sets of 3-4 fields of GFP fluorescence images for *S. cerevisiae* interacting protein pairs and negative controls. All fields are shown at the same magnification.

A

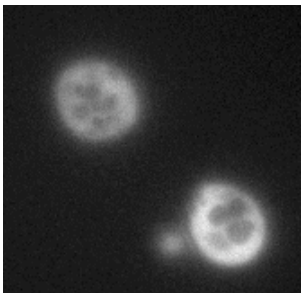

B

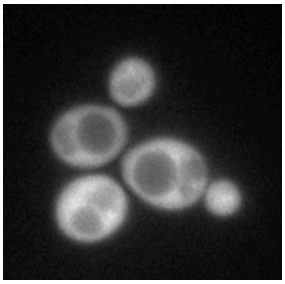

C

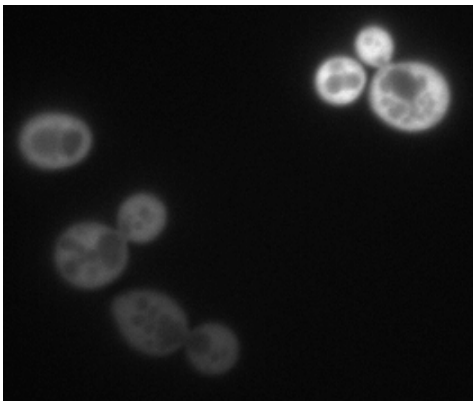

FIGURE S7.— *S. cerevisiae* SNF1GFP & SNF4VPS32 WT. Sets of 3-4 fields of GFP fluorescence images for *S. cerevisiae* interacting protein pairs and negative controls. All fields are shown at the same magnification.

A

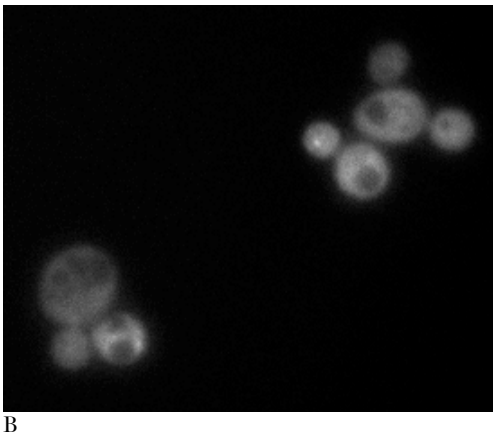

B

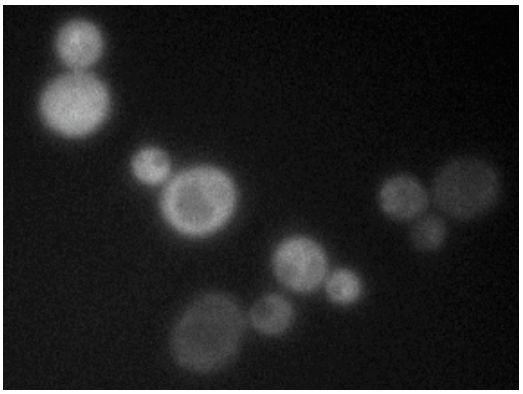

C

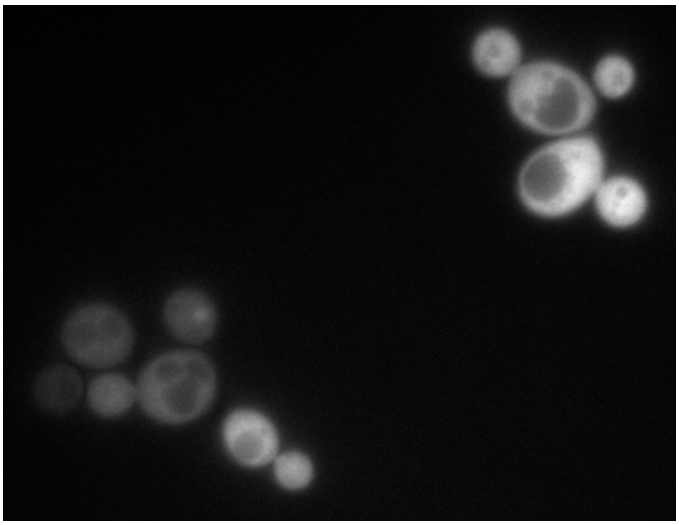

FIGURE S8.— *S. cerevisiae* SNF1GFP & VPS32 WT. Sets of 3-4 fields of GFP fluorescence images for *S. cerevisiae* interacting protein pairs and negative controls. All fields are shown at the same magnification.

A

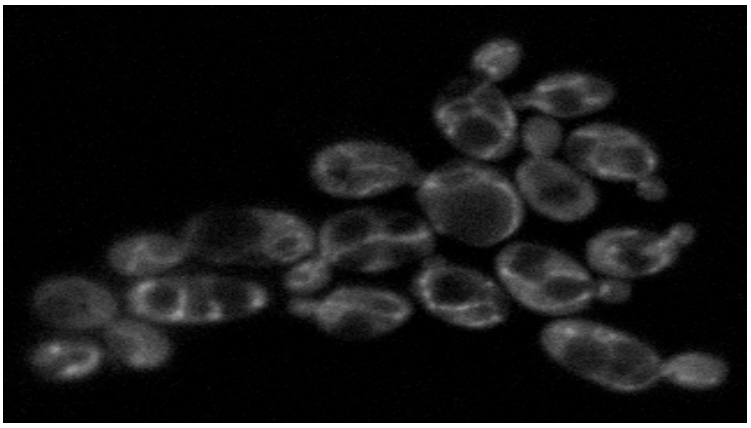

B

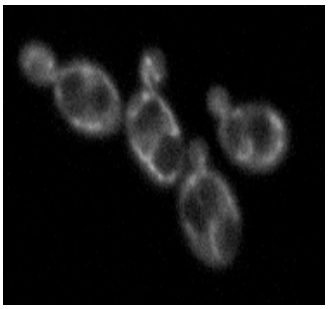

C

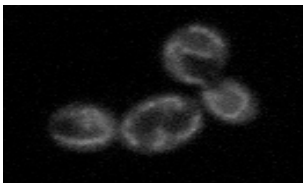

D

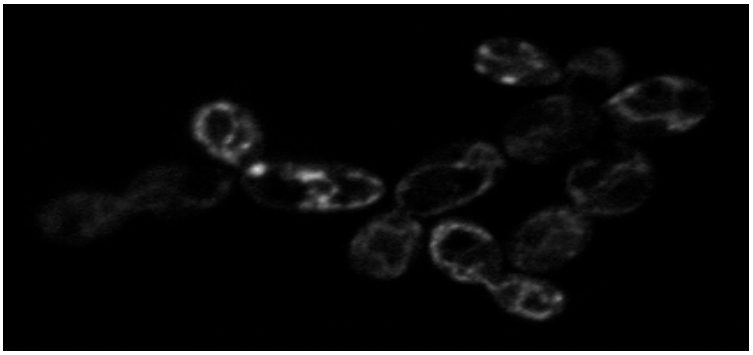

FIGURE S9.— *C. albicans* vps4/vps4 PBS2.GFP&HOG1.VPS32. Sets of 3-4 fields of GFP fluorescence images for *C. albicans* interacting protein pairs and negative controls. All fields are shown at the same magnification.

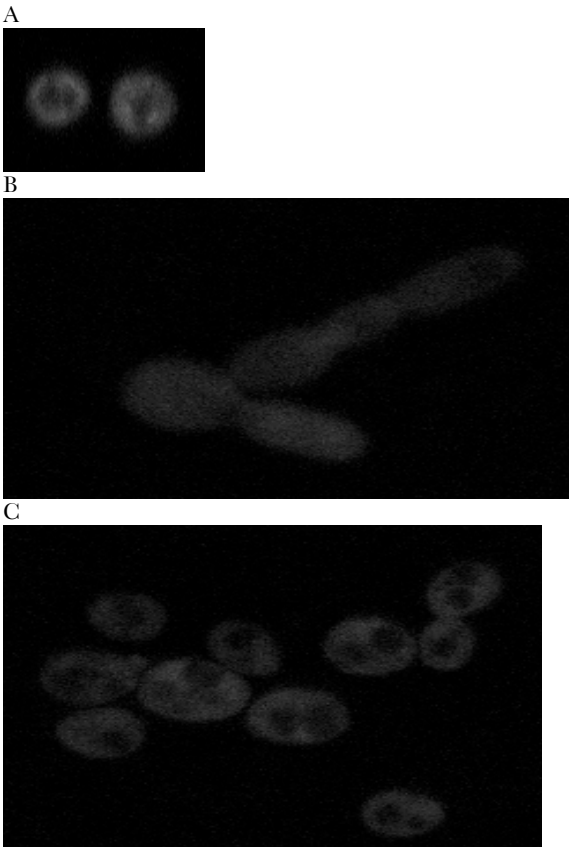

FIGURE S10.— *C. albicans* vps4/vps4 PBS2.GFP&VPS32 EMPTY VECTOR. Sets of 3-4 fields of GFP fluorescence images for *C. albicans* interacting protein pairs and negative controls. All fields are shown at the same magnification.

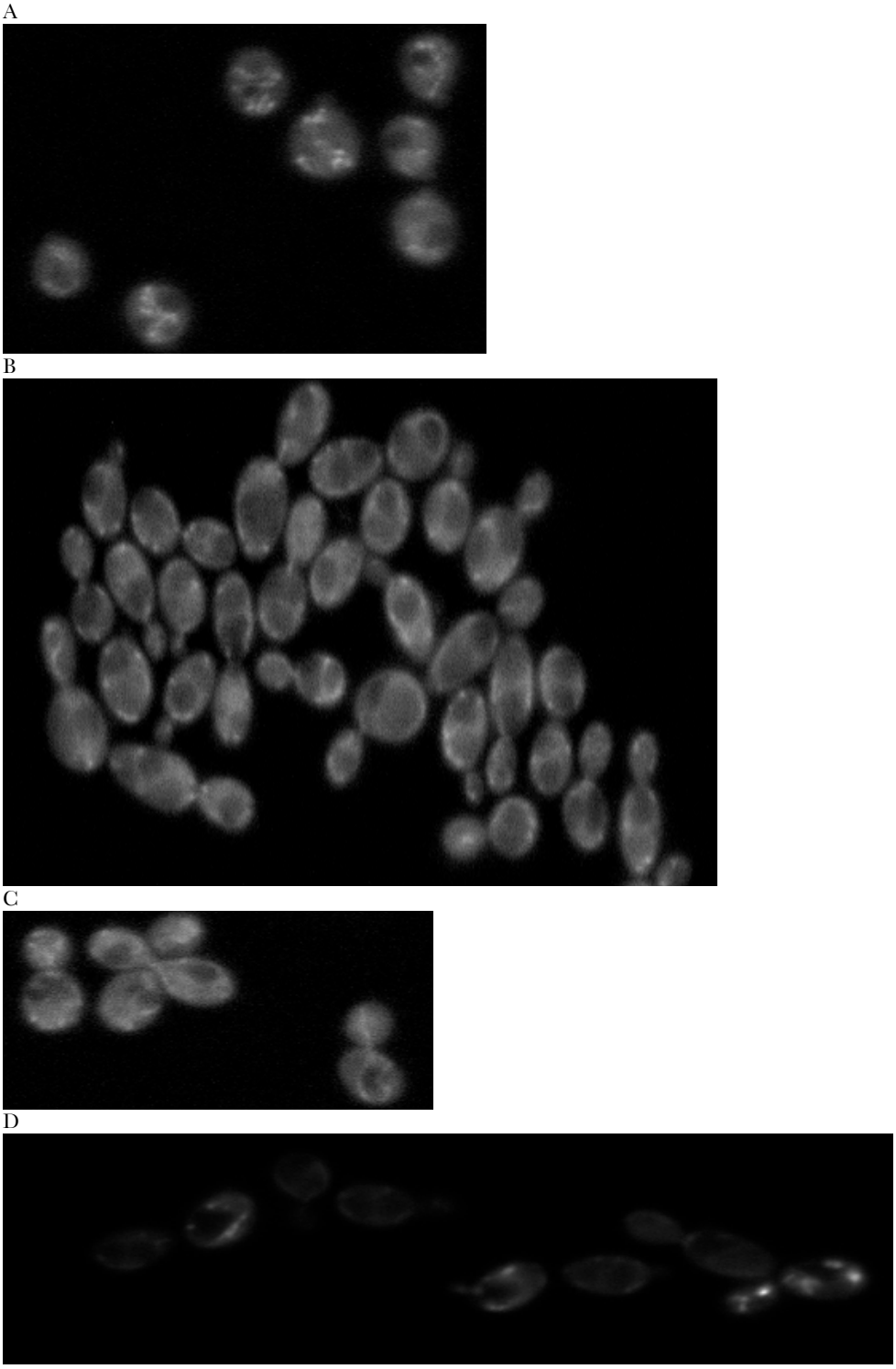

FIGURE S11.— *C. albicans* vps4/vps4 SNF1.GFP&SNF4.VPS32. Sets of 3-4 fields of GFP fluorescence images for *C. albicans* interacting protein pairs and negative controls. All fields are shown at the same magnification.

A

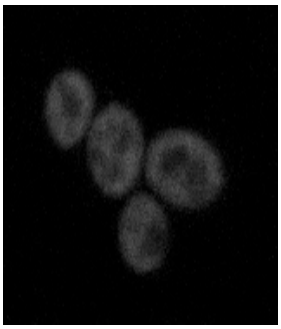

B

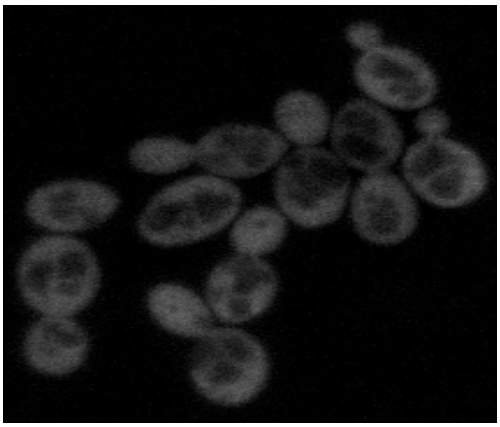

C

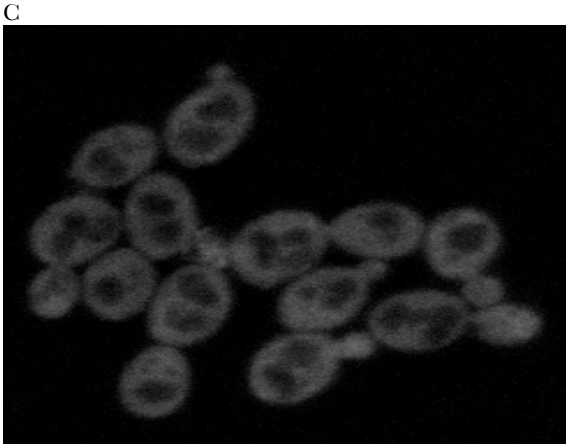

D

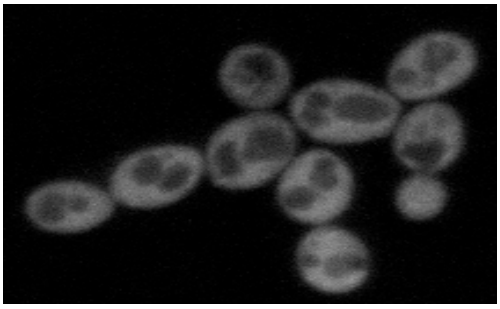

FIGURE S12.— *C. albicans* vps4/vps4 SNF1.GFP&VPS32 EMPTY VECTOR. Sets of 3-4 fields of GFP fluorescence images for *C. albicans* interacting protein pairs and negative controls. All fields are shown at the same magnification.

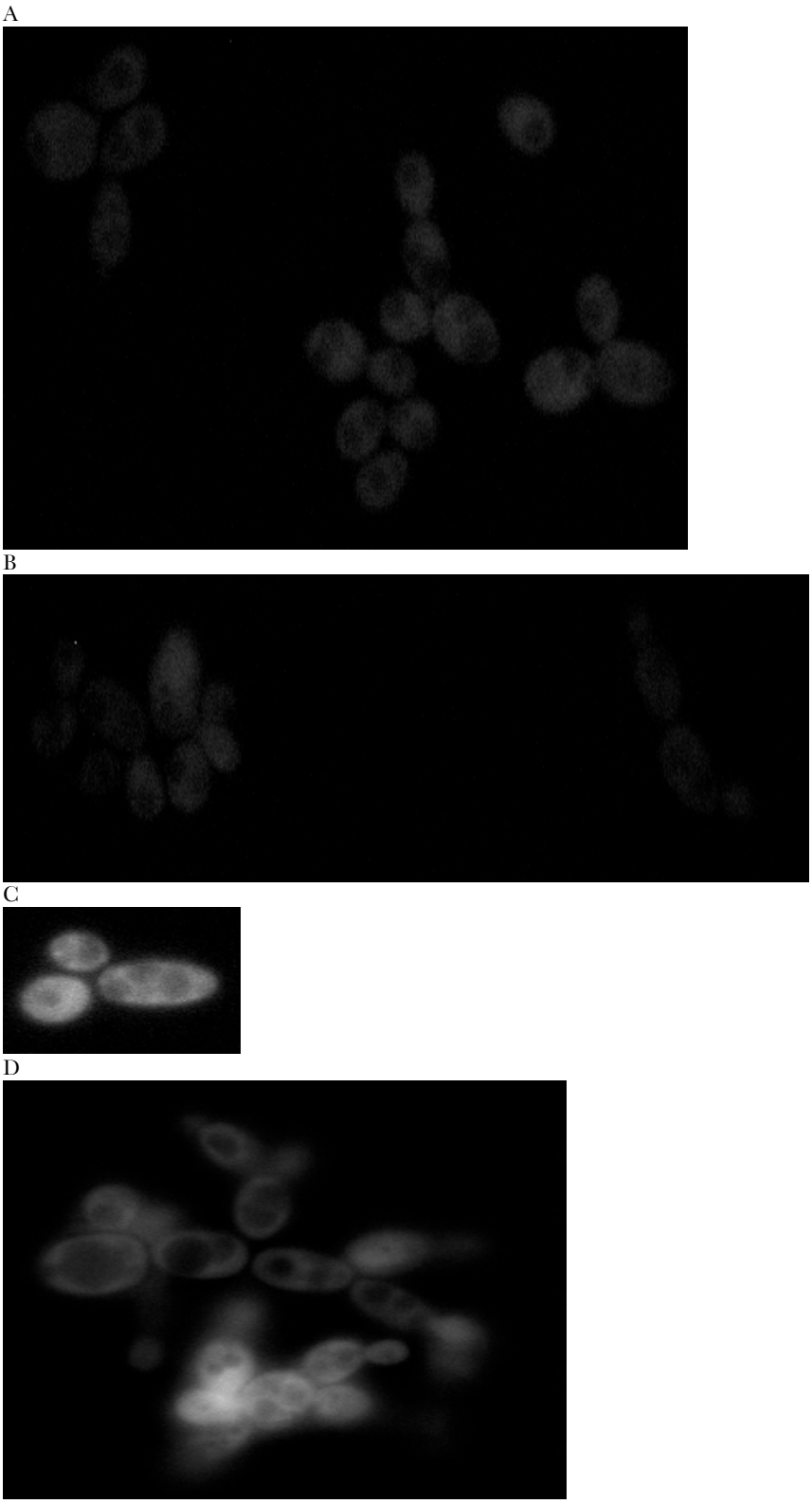

FIGURE S13.— *C. albicans* vps4/vps4 Non Interacting Pairs Control PBS2GFP&SNF4VPS32. Sets of 3-4 fields of GFP fluorescence images for *C. albicans* interacting protein pairs and negative controls. All fields are shown at the same magnification.